Fuzzy control of spark advance by ion current sensing

A H Shamekhi* and **A Ghaffari**
Faculty of Mechanical Engineering, K. N. Toosi University of Technology, Tehran, Iran

The manuscript was received on 19 July 2004 and was accepted after revision for publication on 29 September 2006.

DOI: 10.1243/09544070D13504

Abstract: The desired performance of a spark ignition (SI) engine is highly related to the position of the spark advance, and consequently to the beginning of stable combustion inside the cylinder. The magnitude of the generated ion current signal, measured by a sensor inside cylinder, is closely correlated to the cylinder pressure magnitude. Their maximum values almost coincide at the same crank angle position. In this paper, a feedback control system is designed to fix the position of the maximum pressure at a given desired value of the crank angle. Noting that SI engines are highly non-linear systems, a fuzzy logic controller is developed. The simulation results present a quite satisfactory performance of the closed-loop system.

Keywords: fuzzy logic controller, ionization current, peak pressure position, spark advance, SI engines

1 INTRODUCTION

The last generation of vehicle engines is mainly controlled by engine management systems (EMS). These types of engine are either open-loop or closed-loop control systems. In an open-loop type, the engine test results on test beds are tabulated in the form of look-up tables for different operational conditions. The look-up table is saved on the microcontroller unit of the EMS [**1**]. An essential variable in the performance of spark ignition (SI) engines is the ignition timing. Different parameters such as engine speed, manifold pressure, manifold temperature, inlet air temperature, air–fuel ratio, fuel characteristics, exhaust gas recirculation (EGR), coolant temperature and humidity, affect the optimal ignition timing [**2**]. In today's production lines, the ignition timing is mostly controlled by an open-loop scheme that relies on a look-up table. The look-up tables are calibrated through extensive experiments in either an engine test bed or chassis dynamometer. These are essentially open loop-control commands. Consequently, any changes in the parameters of the system or in the environmental conditions cause the system to deteriorate from its optimal condition. The more intensive emission regulations in the future and the high market demand for lower fuel consumption leads researchers to substitute the existing open-loop control systems with modified closed-loop optimal controls. Two methods, among the others, are presented to keep the peak pressure at a fixed position of the crank angle. In the first method the cylinder pressure is directly measured, while in the second method the ionization current is measured inside the cylinder. A variety of cylinder-pressure-based engine control systems have been reported in the literature [**3–7**]. However, they have not been yet proven to be cost effective due to the high cost of pressure sensors and limited durability considerations of these sensors.

The most common types of cylinder pressure sensors are intrusive devices that are packaged through the combustion chamber wall [**8–11**]. Ion current signal sensors, on the other hand, are the best substitute for pressure sensors [**12**]. An ion current signal can be measured with a spark plug. This signal is used in knock control, misfire detection, air–fuel ratio, and spark advance control systems [**12–20**]. In this paper, a feedback control system is designed to fix the position of maximum pressure at a given desired value of the crank angle, based on the measurements of ion currents.

** Corresponding author: Faculty of Mechanical Engineering, K. N. Toosi University of Technology, Vafadar-e-Sharghi Street, 4th Square, PO Box 016765 3381, Tehran 16579, Iran. email: shamekhi@me.kntu.ac.ir*

d000003504 11-12-06 11:13:55 Rev 14.05
The Charlesworth Group, Wakefield 01924 204830

2 THEORY AND FORMULATION

2.1 The ion generating process

The ionization process may briefly be described as follows: the heat in the flame front ionizes the gas in the combustion chamber and the gas becomes conductive. An electrical field is then generated in the combustion chamber and the current is measured. The ionization current contains information about the combustion process and pressure. The following equation is an example of an ideal reaction in an internal combustion engine

$$C_8H_{18} + \frac{25}{2}O_2 \rightarrow 8\,CO_2 + 9\,H_2O \tag{1}$$

However, the actual combustion process has several stages. The high temperature inside the cylinder ionizes the molecules. The ionized molecules are recombined and more stable molecules are generated. Some preliminary reactions are included in the ion creation

$$\begin{aligned} &CH + O \rightarrow CHO^+ + e^- \\ &CHO^+ + H_2O \rightarrow H_3O^+ + CO \\ &CH + C_2H_2 \rightarrow C_3H_3^+ + e^- \end{aligned} \tag{2}$$

The generated ions are not limited to those in equation (2). Other ions such as $C_3H_3O^+$, OH^-, O^{2-}, and a considerable amount of H_3O^+ and $C_3H_3^+$ are also generated. These positive ions and electrons become carriers of ionic currents [**14**]. To measure the degree of ionization, a probe is inserted into the combustion chamber. The probe is biased in order to create an electrical field that attracts and rejects ions in the vicinity of the probe.

In Fig. 1 the ionization signal is displayed as a function of crank angle. It has three phases: ignition, flame front, and post flame [**20**].

2.2 Ionization current modelling

An analytical expression for the ionization current has been presented, assuming that the gas in the spark plug is fully combusted and in thermodynamic equilibrium also assuming that the current is carried in a cylinder extending from the central electrode of the spark plug. Given the cylinder pressure and temperature the analytical expression for the ionization current is

$$I = A x_i^{1/2} P^{-1/2} T^{3/4} \exp\left(-\frac{E_i}{2\sigma T}\right) \tag{3}$$

where A is a constant.

Figure 2 shows the variation of ion current during the post flame period. The relative current may be written as

$$\frac{I}{I_{\max}} = \left(\frac{x_i}{x_{i\,\max}}\right)^{1/2} \left(\frac{P}{P_{\max}}\right)^{-1/2} \left(\frac{T}{T_{\max}}\right)^{3/4} \exp(BB) \tag{4}$$

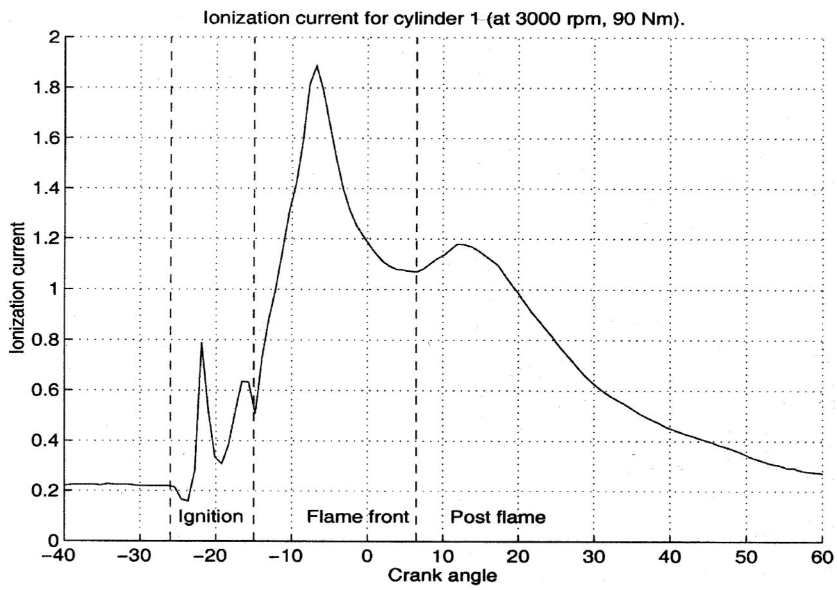

Fig. 1 Ionization current signal characteristic in three phases: ignition, flame front and post flame [**20**]

d000003504 11-12-06 11:13:55 Rev 14.05
The Charlesworth Group, Wakefield 01924 204830

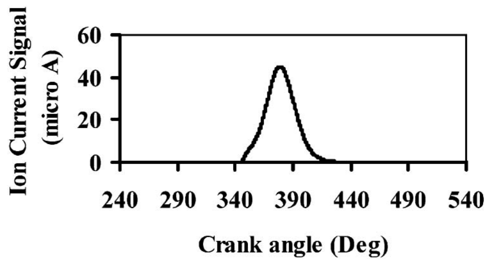

Fig. 2 Ion current variation in the post flame period (simulation)

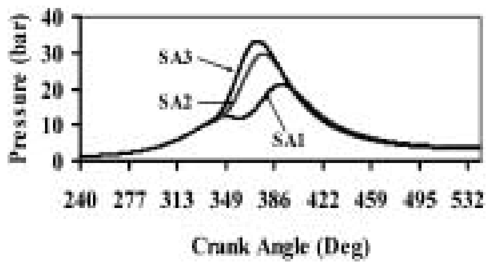

Fig. 3 Three different pressure traces, resulting from three different spark timings: SA1 = 15°, SA2 = 25°, SA3 = 30°BTDC (simulation)

where

$$BB = -\frac{E_i}{2\sigma T_{\max}}\left[\left(\frac{T_{\max}}{T}\right) - 1\right] \tag{5}$$

and the quantities $T_{\max}$, $P_{\max}$, and $x_{\max}$ are the temperature, pressure, and total density at $I_{\max}$ [**21**].

3 SPARK ADVANCE CONTROL

Spark advance control deals with controlling the appropriate timing of the spark plug ignition inside the cylinder. The engine efficiency and emissions are directly affected by the spark advance. Therefore the ignition time is selected to maximize the engine power, while avoiding the engine knock and emission increase. The best spark advance setting for an internal combustion engine depends on the engine load, speed, air temperature, and air–fuel ratio. Other variables and parameters have a minor effect on the spark advance position. Nowadays, the spark control systems measure some of these parameters and adjust them based on extensive engine testing during the design period. However, it is very difficult to measure all parameters and would be extremely expensive and time consuming to perform the engine testing required by mapping the effects of all the parameters on the spark. The use of ion current base spark control is a fundamentally different approach that relies on feedback and has the potential to reduce the amount of calibration required for a new engine design. Compared with the open-loop control systems (look-up tables) it also improves the engine's efficiency under large variations of the actual operating conditions.

3.1 Spark advance, cylinder pressure, and ion current

In Fig. 3 three different pressure traces are shown for three different spark timings. Earlier spark advance gives higher maximum pressure and temperature. With too early ignition timing the pressure rise starts too early and counteracts the piston movement. Too late ignition gives a pressure increase that comes too late, so that work is lost during the expansion stroke. Under normal driving conditions the mixture is ignited around 15–30° before top dead centre (BTDC) and the pressure peak comes around 20° after top dead centre (ATDC).

To define the position of the cylinder pressure relative to TDC, the peak pressure position (PPP) is used (Fig. 4). The PPP for maximum output torque lies around 16° after TDC for all these operating points. Hubbard *et al.* show that a spark schedule that maintains a constant PPP at 16° is close to optimum [**3**]. This method is used and is validated by many researchers [**3–7**].

The simulation results show that the maximum value of the generated ion current during the post flame period coincide with the peak pressure position. This result is shown in Fig. 5 [**21**]. Similar experimental test results are shown in Fig. 6 [**20**].

3.2 Controller design

It is proposed to design a controller such that it maintains the peak pressure at a fixed position, namely 16° after TDC. Note that SI engines are highly non-linear systems and unmodelled dynamics are always confronted. Therefore, a fuzzy logic controller (FLC) is developed and designed for this system. This type of digital controller is suitable for non-linear

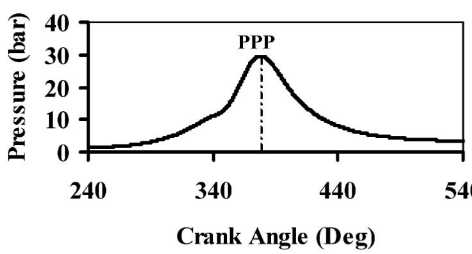

Fig. 4 Cylinder pressure and PPP verses crank angle (simulation)

d000003504 11-12-06 11:13:55 Rev 14.05
The Charlesworth Group, Wakefield 01924 204830

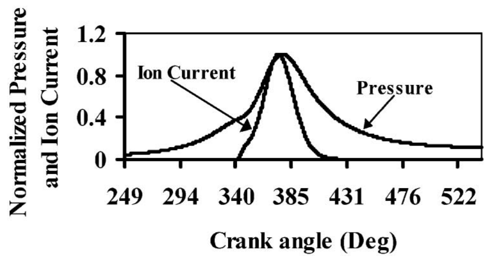

Fig. 5 Normalized ion current and pressure variation via crank angle (simulation)

systems and are also robust to noise and parameter variations [**22**, **23**]. Figure 7 shows the block diagram of this feedback control system with a fuzzy logic controller.

The designed FLC is a multi-input–single-output controller. Error and error derivative signals are inputs and C is the controller output signal. The error signal (e) is the difference between the desired position of peak pressure $(\mathrm{PPP})_{\mathrm{ref}}$ and its measured value (PPP). It should be noted that in this system the generated ion current is measured instead of the pressure of the cylinder using a pressure sensor.

In Fig. 7, the error signal is given by the relation

$$e = (\mathrm{PPP})_{\mathrm{ref}} - \mathrm{PPP} \tag{6}$$

In this paper the quantity PPP is calculated from the engine dynamical model [**24**]. The error derivative signal is calculated by the relation

$$\dot{e}(t) = \frac{e(t) - e(t - \Delta t)}{\Delta t} \tag{7}$$

where Δt is the time interval between two sequential spark advances. A proportional-integral (PI) action control law has been used to eliminate the system offset (steady state error). The control law is

$$\mathrm{SA}(n+1) = \mathrm{SA}(n) - C[\mathrm{PPP}_{\mathrm{ref}}(n) - \mathrm{PPP}(n)] \tag{8}$$

where C is a constant gain between 0.0 and 1.0, and should be tuned by the fuzzy logic controller.

3.3 The structure of the fuzzy logic controller

The fuzzy logic controller consists of five sections: fuzzifier, data base, rule base, inference mechanism, and defuzzifier (Fig. 8). The fuzzifier changes the

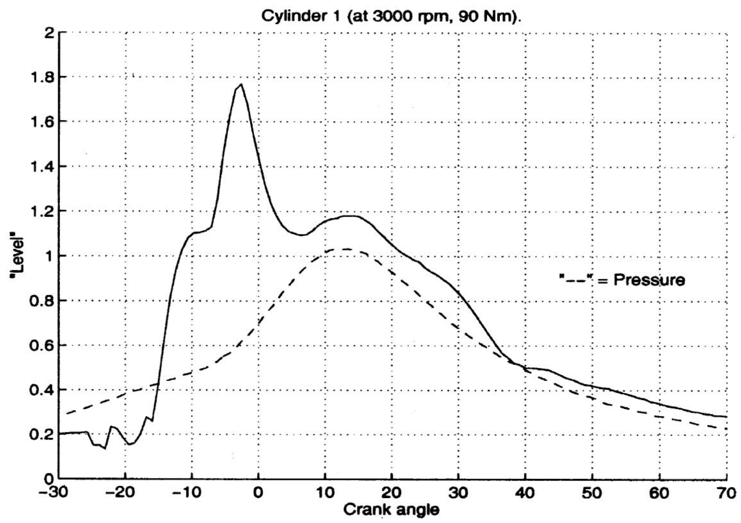

Fig. 6 Ion current and pressure variation via crank angle (experimental) [**20**]

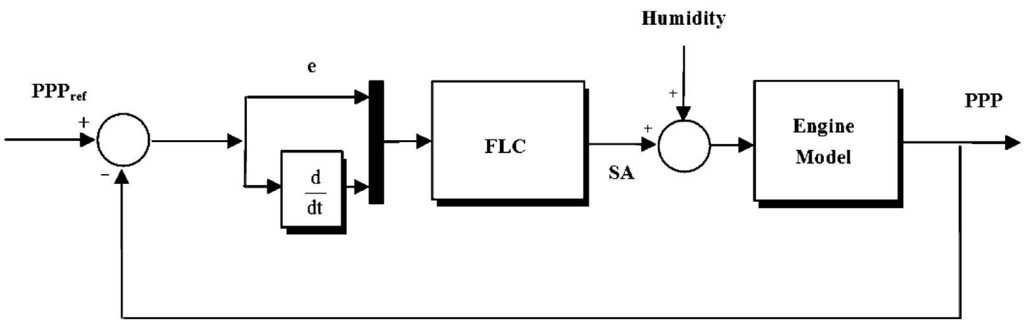

Fig. 7 Block diagram of the control system

d000003504 11-12-06 11:13:55 Rev 14.05
The Charlesworth Group, Wakefield 01924 204830

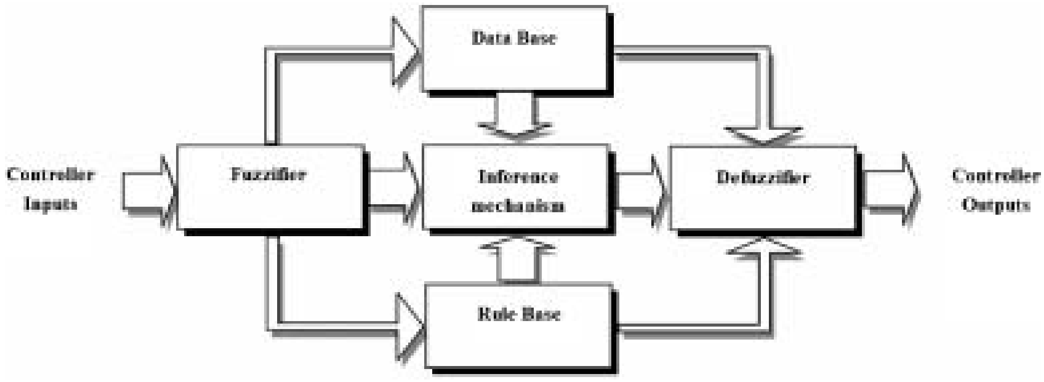

Fig. 8 Fuzzy logic controller structure

crisp variables (e) and ($\dot{e}$) into singleton fuzzy sets. If the fuzzy set, E, is a fuzzy singleton, then

$$\mu_E(s) = \begin{cases} 1.0 & \text{if } s = e \\ 0 & \text{otherwise} \end{cases} \quad (9)$$

The ith IF–THEN rule of the fuzzy controller rule base has the structure

$$R_i: \text{IF } (e \text{ is } E_j) \text{ and } (\dot{e} \text{ is } \dot{E}_k) \text{ THEN } (c \text{ is } C_p)$$
$$\text{for } j = 1, 2, \ldots, 7; k = 1, 2, \ldots, 7; p = 1, 2, \ldots, 7 \quad (10)$$

where R_i ($i = 1, 2, I$) is the ith rule and I is the total number of rules. The variables e, $\dot{e}$, and c are linguistic variables and E_j, E_k, and C_p are primary fuzzy sets. They have been partitioned into seven parts

{NB, NM, NS, ZE, PS, PM, PB}

The maximum number of rules is 49. The fuzzy rules in the rule base are listed in Table 1.

In this paper normalized triangular membership functions are used (Fig. 9). The Inference mechanism is a fuzzy reasoning engine that is composed of fuzzy approximative rules and compositional operators. In this paper the fuzzy approximative minimum rule and the Sup-min compositional operator are used [**23**].

Table 1 The rule base of the fuzzy controller

$\dot{e}/e$	NB	NM	NS	ZE	PS	PM	PB
NB	PB	PB	PB	PB	PM	PM	PS
NM	PB	PM	PM	PM	PS	PS	ZE
NS	PM	PM	PS	PS	PS	ZE	ZE
ZE	PS	PS	PS	ZE	NS	NS	NM
PS	ZE	ZE	NS	NS	NM	NM	NM
PM	ZE	NS	NM	NM	NM	NB	NB
PB	NM	NB	NB	NB	NB	NB	NB

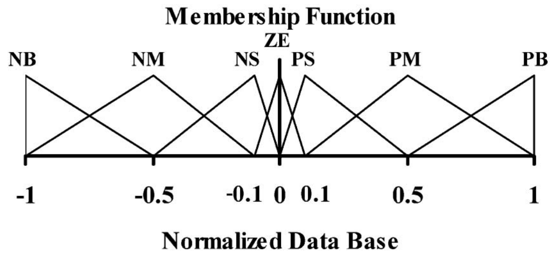

Fig. 9 Normalized data base

The fuzzy inference minimum rule can be written as

$$R_i = E_j \times \dot{E}_k \times C_p = \int_{E,\dot{E},C} \text{Min}[\mu_{E_j}(e) \circ \mu_{\dot{E}_k}(\dot{e}) \cdot \mu_{C_p}(c)]/(e, \dot{e}, c) \quad (11)$$

and the Sup-min compositional operator can be described as

$$C =: (E \times \dot{E}) \circ R_i = \int_C \text{Sup}\{E, \dot{E}\} \text{ Min}[\mu_{E \times \dot{E}}(e, \dot{e}) \cdot \mu_{E_j \times \dot{E}_k \times C_p}(e, \dot{e}, c)]/c \quad (12)$$

where the values of $\mu_{E \times \dot{E}}(e, \dot{e})$ and $\mu_{E_j \times \dot{E}_k \times C_p}(e, \dot{e}, c)$ can be obtained by fuzzy rules and fuzzy inference. The crisp output is obtained via the process of defuzzification. For defuzzification, the centre of the area is considered

$$c = \frac{\sum_{i=1}^{7} c_f \mu_{C_p}(c_f)}{\sum_{i=1}^{7} \mu_{C_p}(c_f)} \quad (13)$$

3.4 Disturbance rejection

In SI engines, humidity is one of the major external disturbances that affects the pressure and ion current signals. In order to evaluate the performance of the

d000003504 11-12-06 11:13:55 Rev 14.05
The Charlesworth Group, Wakefield 01924 204830

closed-loop control system at the presence of an external disturbance, an air humidity model is proposed. Firstly, the air humidity model will be proposed and then the controller behaviour will be investigated.

3.5 Air and humidity mixture model

In this section a model of the air and humidity mixture is investigated based on the following assumptions [**25**]:

1. There is no dissolved gas in the air.
2. The gaseous phase can be treated as a mixture of the ideal gas.
3. When equilibrium is achieved, the partial pressure of the vapour is equal to the saturation pressure corresponding to the temperature of the mixture.

By defining the relative humidity (φ) as the ratio of the mole fraction of the vapour in the total pressure and the humidity ratio (κ) as the ratio of the mass of vapour (m_v) to the mass of dry air (m_a), then

$$\varphi = \frac{P_v}{P_g} \tag{14}$$

and

$$\kappa = \frac{m_v}{m_a} \tag{15}$$

Therefore

$$\varphi = \frac{\kappa P_a}{0.622 P_g} \tag{16}$$

By referring to the above relations the mole fraction of the humidity of the mole of oxygen in the air mixture (ζ) is defined as

$$\zeta = 4.9749 \varphi \frac{P_g}{P_a} \tag{17}$$

4 SIMULATION RESULTS

In this section the simulation results of the fuzzy logic controller for optimal spark advance control are proposed. In Fig. 10 the spark advance variation in the presence of the air humidity is shown. As seen in Fig. 10, the controller output can reach the desired spark advance after 7 cycles. Figure 11 shows how the controller achieves the desired peak pressure position.

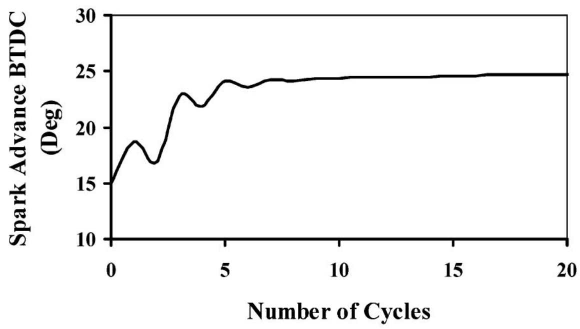

Fig. 10 Spark advance variation via number of cycles in the presence of disturbance (simulation)

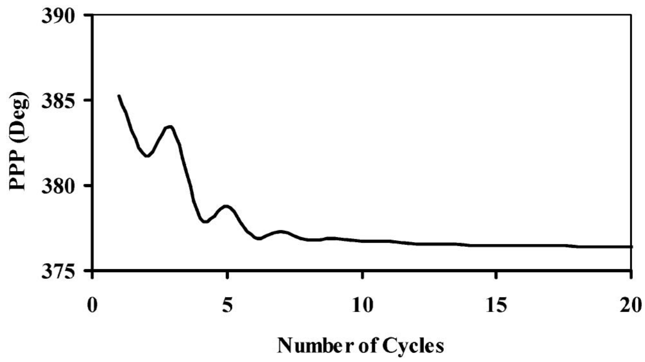

Fig. 11 Peak pressure position variation via number of cycles in the presence of disturbance (simulation)

5 CONCLUSION

In this paper the ionization current during the post flame combustion period and the correlation between the cylinder pressure and ion current signal are investigated. Based on relations between spark advance and pressure and ion current development a fuzzy logic controller is designed for optimal spark advance control. Simulation results show the excellent performance of the controller and its robustness in the presence of disturbances.

REFERENCES

1 **Adler, U.** *Automotive electric/electronic systems*, 5th Edition, 2000 (Robert Bosch GmbH).
2 **Heywood, J. B.** *Internal combustion engine fundamentals*, McGraw-Hill Series in Mechanical Engineering, 1988 (McGraw-Hill).

d000003504 11-12-06 11:13:55 Rev 14.05
The Charlesworth Group, Wakefield 01924 204830

3 **Hubbard, M., Dobson, P. D.,** and **Powell, J. D.** Closed loop control of spark advance using a cylinder pressure sensor. *Trans. ASME, J. Dynamic Systems, Measmt, and Control*, 1978, 414–420.
4 **Glaser, I.** and **Powell, J. D.** Optimal closed-loop spark control of an automotive engine. SAE paper 810058, 1981.
5 **Powell, J. D.** Engine control using cylinder pressure: past, present, and future. *Trans. ASME, J. Dynamic System, Measmt, and Control*, 1993, **115**, 343–350.
6 **Muller, R.** and **Hemberger, H. H.** Neural adaptive ignition control. SAE paper 981057, 1998.
7 **Isermann, R.** and **Muller, N.** Nonlinear identification and adaptive control of combustion engines. In IFAC, 2001.
8 **Anastasia, C. M.** and **Pestana, G. W.** A cylinder pressure sensor for closed loop engine control. SAE paper 870288, 1987.
9 **Pestana, G. W.** Engine control methods using combustion pressure feedback. SAE paper 890758, 1989.
10 **Yoon, P., Park, P., Sunwoo, M., Ohm, I.,** and **Yoon, K. J.** Closed-loop control of spark advance and air–fuel ration in SI engines using cylinder pressure. SAE paper 2000-01-0933, 2000.
11 **Sellnau, M. C., Matekunas, F. A., Battiston, P. A., Chang, C. F.,** and **Lanchester, D. R.** Cylinder-pressure-based engine control using pressure-ratio-management and low-cost non-intrusive cylinder pressure sensors. SAE paper 2000-01-0932, 2000.
12 **Shamekhi, A. H.** and **Ghaffari, A.** Peak pressure position estimation by ion current sensing. In the 10th ISME International Conference of Mechanical Engineers, 2002, pp. 608–613.
13 **Shimasaki, Y., Kanehito, M., Baba, S., Muaruyama, S., Hisaki, T.,** and **Miyatu, S.** Spark plug voltage analysis for monitoring combustion in an internal combustion engine. SAE paper 930461, 1993.
14 **Auzins, J., Johansson, H.,** and **Nytomt, J.,** Ion-gap sense in misfire detection, knock and engine control. SAE paper 950004, 1995.
15 **Lee, A.** and **Pyko, J. S.** Engine misfire detection by ionization current monitoring. SAE paper 950003, 1995.
16 **Reinmann, R., Saitzkoff, A.,** and **Mauss, F.** Local air–fuel ratio measurements using the spark plug as an ionization sensor. SAE paper 970856 (SAE SP-1263), 1997, pp. 175–185.
17 **Shamekhi, A. H.** and **Ghaffari, A.** Spark advance control by ion current sensing in SI engines. In the 11th ISME International Conference of Mechanical Engineers, 2003, pp. 1908–1914.
18 **Malaczynski, G. W.** and **Baker, M. E.** Real time digital signal processing of ionization current for engine control diagnostic and control. SAE technical paper series 2003-01-1119, 2003.
19 **Wang, Y.** and **Zhou, L.** Investigation of the detection of knock and misfire of a spark ignition engine with the ionic current method. *Proc. Instn Mech. Engrs, Part D: J. Automobile Engineering*, **217**(D7), 2003, 617–621.
20 **Eriksson, L., Nielsen, L.,** and **Nytomt, J.** Ignition control by ionization current interpretation. SAE paper 960045, 1996.
21 **Shamekhi, A. H.** and **Ghaffari, A.** Ion current simulation during the post flame period. Accepted for publication in *IRANIAN J. of Chemistry and Chemical Engineering*.
22 **Shamekhi, A. H.** and **Ghazavi, A.** Fuzzy control of a flexible robot arm constructed from graphite/epoxy. In the 10th ISME International Conference of Mechanical Engineers, 2002, pp. 84–91.
23 **Wang, Lie-Xin** *A course in fuzzy systems and control*, 1997 (Prentice Hall, Englewood Cliffs, New Jersey).
24 **Shamekhi, A. H.** and **Gaffari, A.** An improved model for SI engines. ASME paper ICEF2004-818, 2004.
25 **Sonntag, R., Borgnakke, C.,** and **Van Wylane, G. J.** *Fundamentals of thermodynamics*, 6th Edition, 2003 (John Wiley & Sons, Ltd, Chichester, West Sussex).

APPENDIX

Notation

e	error signal
$\dot{e}$	derivative of the error signal
E	reference set of error signal
$\dot{E}$	reference set of derivative of error signal
E_i	ionization energy (eV)
EGR	exhaust gas recirculation
FLC	fuzzy logic controller
I	electrical current (A)
MBT	maximum brake torque (N m)
NB	negative big
NM	negative medium
NS	negative small
P	pressure (Pa)
PI	proportional and integral
PPP	peak pressure position (deg)
PB	positive big
PM	positive medium
PS	positive small
SA	spark advance (deg)
T	temperature (K)
TDC	top dead centre
x_i	mole fraction of i species
ZE	zero
ζ	mole fraction of humidity to the mole of oxygen in the air mixture
κ	humidity ratio
λ	membership function

d000003504 11-12-06 11:13:55 Rev 14.05
The Charlesworth Group, Wakefield 01924 204830

σ	Boltzmann's constant (J/K molecule)
φ	relative humidity
ω_e	engine speed (rad/s)

Subscripts

a	air
est	estimated
f	fuzzy
g	gas
max	maximum
min	minimum
ref	reference
sup	suprimum
v	vapour

d000003504 11-12-06 11:13:55 Rev 14.05
The Charlesworth Group, Wakefield 01924 204830